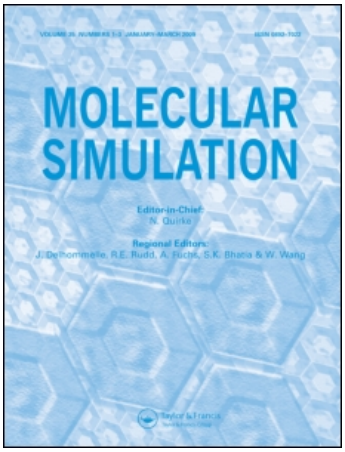

Molecular Simulation
Publication details, including instructions for authors and subscription information:
http://www.informaworld.com/smpp/title~content=t713644482

Numerical modeling of experimentally fabricated InAs/GaAs quantum rings

I. Filikhin[a]; E. Deyneka[a]; B. Vlahovic[a]
[a] Department of Physics, North Carolina Central University, Durham, NC, USA

To cite this Article Filikhin, I. , Deyneka, E. and Vlahovic, B.(2007) 'Numerical modeling of experimentally fabricated InAs/GaAs quantum rings', Molecular Simulation, 33: 7, 589 — 592
To link to this Article: DOI: 10.1080/08927020601067516
URL: http://dx.doi.org/10.1080/08927020601067516

Molecular Simulation, Vol. 33, No. 7, June 2007, 589–592

Taylor & Francis
Taylor & Francis Group

Numerical modeling of experimentally fabricated InAs/GaAs quantum rings

I. FILIKHIN*, E. DEYNEKA† and B. VLAHOVIC

Department of Physics, North Carolina Central University, 1801 Fayetteville Street, Durham, NC 27707, USA

(Received June 2006; in final form October 2006)

Single sub-band model for InAs/GaAs quantum rings (QR), with the electron effective mass dependent on the confinement energy by the Kane formula is applied for numerical simulation of the capacitance-voltage (CV) spectroscopy experiments. Geometrical parameters chosen for the model are based on the fabrication process for InAs/GaAs QD/QR. The 3D confined energy problem is solved numerically by the finite element method. Obtained results for QR single energy levels are in a good agreement with CV measurements. Evaluated magnitude of the electron effective mass is correlates with the FIR spectroscopy data. These results are compared with the existing 2D model calculations. Theoretical estimates for the addition to a ground state energy of the QR in external magnetic field are given, and compared with the experimental CV data.

Keywords: Quantum dots; Electron levels; Single tunneled electron; Spectroscopy

1. Introduction

Successful fabrication of nano-sized self-assembled quantum dots (QD) and quantum rings (QR) with controlled geometrical properties has highlighted their potential for practical photonic device applications. Well-established process of QD formation by the epitaxial growth and their consecutive transformation into the QR [1,2] allow manufacturing of 3D structures with the lateral size about 40–60 nm, and the height of 2–8 nm. It is now possible to directly observe discreet energy spectra of QD and QR by the capacitance-voltage (CV) and far infrared (FIR) spectroscopy [1–3]. Related theoretical studies, however, applied either the 2D models, or 3D models that were not related to the actual QR fabrication sizes and experimental conditions, therefore having some limitations while interpreting experiments [2–6].

In the presented work a single sub-band model for InAs/GaAs QD (QR) is applied, where the electron effective mass is depending on the confinement energy by the Kane formula [7]. Geometrical parameters of the model are based on the fabrication process for InAs/GaAs QD/QR, for which the experimental CV and FIR data is available [1–3]. We assume that the QD to QR transformation occurs without essential diffusion of GaAs substrate material into the InAs QR. For geometry configuration of the QR a model suggested by Blossey and Lorke [8] was employed. The 3D confined energy problem [9–10] was solved numerically by the finite element method (FEM) using iterative procedure. Experimental single electron spectra taken from the CV measurements [2,3] were applied in order to define the additional QR potential, effectively simulating a total contribution of the band-gap deformation potential, the strain induced potential, and the piezoelectric potential [6]. The magnitude of the electron effective mass is compared with the FIR spectroscopy data [3]. These results are accompanied by analysis of the related 2D model calculations [2,3]. Theoretical estimates for the addition to the ground state energy of QR in the external magnetic field are presented, and compared with experimental CV data.

2. Model description

The InAs QRs are considered. QRs having a rotational symmetry are embedded into the GaAs substrate. Geometrical parameters of the QR are the height H, the radial width ΔR, and the inner radius R_1 (the outer radius

*Corresponding author. Email: ifilikhin@nccu.edu
†Present address: Cree Inc., 4600 Silicon Drive, Durham, NC 27703 USA.

Molecular Simulation
ISSN 0892-7022 print/ISSN 1029-0435 online © 2007 Taylor & Francis
http://www.tandf.co.uk/journals
DOI: 10.1080/08927020601067516

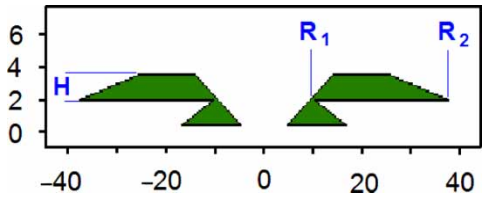

Figure 1. Cross section of the quantum ring.

is $R_2 = R_1 + \Delta R$). A cross section of the QR is shown in figure 1. The following geometrical parameters reported for experimental fabricated QR [1,2,11] were used in the model: $R_1 = 10\,\text{nm}$, $R_2 = 40\,\text{nm}$, $H = 1.5\,\text{nm}$. The previously reported geometry for QD was having $R_1 = 10\,\text{nm}$, $H = 7\,\text{nm}$ [1,2]. The volume of the QR is slightly larger then the volume of the initial QD. We attribute this difference to the insufficient diffusion of the GaAs substrate material into the InAs QR. Presented QR geometry is analogous to the model suggested in Ref. [8].

The 3D heterostructure described above is modeled utilizing the *kp*-perturbation single sub-band approach with the energy-dependent quasi-particle effective mass [9–10,12]. The energies and the wave functions of the single electron in a semiconductor structure are the solutions of the nonlinear Schrödinger equation:

$$\left(-\frac{\hbar^2}{2m^*(x,y,z,E)}\nabla^2 + V(x,y,z) - E\right)\Psi(x,y,z) = 0, \quad (1)$$

where $V(x,y,z)$ is the band gap potential, proportional to energy misalignment of the conduction band edges of InAs QR and GaAs substrate. The electron effective mass $m^* = m^*(x,y,z,E)$ is defined by the Kane formula [7] for each area of the QR/Substrate:

$$\frac{m_0}{m^*} = \frac{2m_0P^2}{3\hbar^2}\left(\frac{2}{E_g+E} + \frac{1}{E_g+\Delta+E}\right). \quad (2)$$

Here m_0 is free electron mass, P is Kane's momentum matrix element, E_g is the band gap, and Δ is the spin-orbit splitting of the valence band. E is the ground state confinement energy. $V(x,y,z) = E_0$ inside the substrate, and $V(x,y,z) = 0$ inside the QR. The magnitude of E_0 was calculated as $E_0 = 0.7(E_{g,2} - E_{g,1})$. The boundary conditions for the wave function Ψ on the surface side of the QR are chosen to satisfy the relation: $(\vec{n}, \vec{\nabla}\Psi) = 0$, ($\vec{n}$ where is normal to the surface. The following experimental values [13] were used for the QR (index 1) and the substrate (index 2) components: $(2m_0P_1^2/\hbar^2)/(2m_0P_2^2/\hbar^2) = 20.5/24.6$, $E_{g,1} = 0.42\,\text{eV}$, $E_{g,2} = 1.52$, $\Delta_1 = 0.34\,\text{eV}$, $\Delta_2 = 0.49\,\text{eV}$, $E_0 = 0.77\,\text{eV}$. Bulk effective masses of InAs and GaAs are $m^*_{0,1} = 0.024\ m_0$ and $m^*_{0,2} = 0.067\ m_0$, respectively. The non-linear Schródinger equation (1) is solved by the iterative procedure, where the solution of the linear Schrödinger equation for each step is numerically obtained by the FEM. Details of the numerical treatment were described earlier in Refs. [9,10]. Taking a rotational symmetry of the problem into account, equation (1) can be rewritten in cylindrical coordinates. In this case the energy states are defined by a pair of the quantum numbers (n,l), where $n = 0, 1, \ldots$ and $l = 0, \pm1, \pm2, \ldots$ are the radial and the orbital quantum numbers, respectively.

3. Model with effective potential

That earlier model of QR, which considered only the band-gap potential, could not adequately explain the experimentally observed change in the QR electron effective mass from a bulk value of 0.024 m_0 to the value of 0.063 m_0 [3]. More sophisticated 3D models, with the band-gap deformation potential, the strain-induced potential, and the piezoelectric potential taken into the account, in addition to the band-gap potential, were recently proposed in Ref. [6]. However, a direct comparison of the results [6] and experimental data is not possible because the geometry of QR used in Ref. [6] was far from realistic. In order to improve our prior model [10,12], we have introduced the potential V_s, which simulates an integral effect of all QR potentials listed above, while leaving the realistic geometric parameters intact. The effective potential $V_s \approx 0.5\,\text{eV}$ has attractive character and acts inside a volume of the QR. Feasibility of the corrected model can be tested by comparing the results of our calculations with the exact solution derived in Ref. [6], as shown in figure 2. A cross section of the QR used in our model is depicted in figure 2(a)), and the energies of a few low-lying electronic levels are shown in figure 2(b). One can see that there is a good correlation between the two calculations. The observed small mismatch in values of the energy levels can be attributed to a slight difference between cross sections of the QRs used by both models.

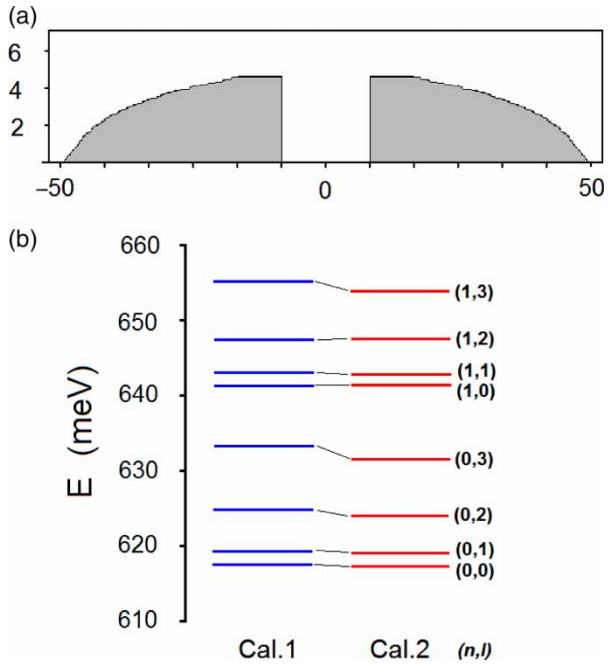

Figure 2. (a) Cross section of the quantum ring. (b) Energies of the lower levels of a single electron spectrum. The *Cal.1* and *Cal.2* relate to the results of our calculations and the ones of [6], respectively. The quantum numbers (n,l) of the electron states are shown.

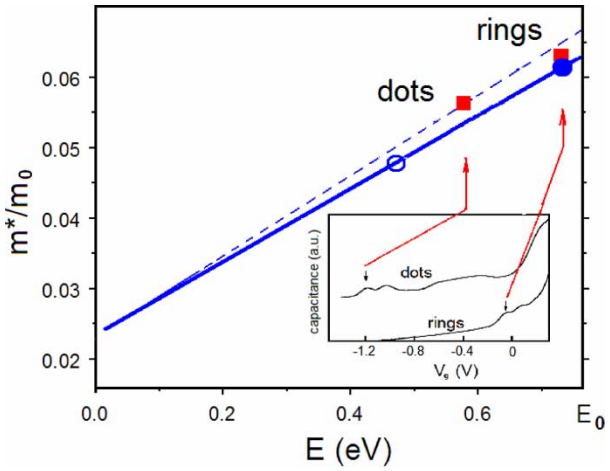

Figure 3. Calculated (circles) and experimentally obtained [1–3] (squares) values for the electron effective mass and s-level energy. Solid line is derived by the Kane formula. Dashed line connects bulk values of the effective mass. The insert: the capacitance-gate-voltage traces [2]. First *s*-levels of QD and QR are shown by arrows. The gate-voltage localization of the *s*-levels in respect to the bottom of the GaAs conduction band is mapped onto the energy scale.

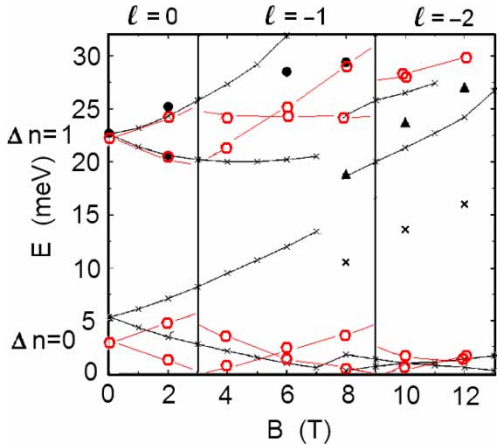

Figure 4. Observed resonance positions [3] of the FIR transmissions at various magnetic field strength B. Calculated energies of the excited states are marked by the open squares. Open circles and small crosses are the results of the present work and calculations of Ref. [3], respectively. The orbital quantum numbers of ground states are shown.

4. Numerical results

The effective potential $V_s = 0.55$ eV was selected for the interpretation of CV experiments. With this correction the electron spectra calculations result in localization of the s-shell electron level in respect to a bottom conduction band of the GaAs substrate, similar to one that can be derived from the CV measurements [2]. The s-level energies and the electron effective masses, calculated with (solid circle) and without (open circle) taking the effective potential into the account, are shown in figure 3. The experimental values for QD and QR are shown as squares for illustration. One can see that the electron effective mass change during the QD to QR transformation is well-reproduced by the Kane's formula. The correlation between the lowest *s*-level of experimental CV data [1] and calculated s-level is shown in figure 3 (Insert). Each peak of the capacitance-gate-voltage traces corresponds to tunneling of a single electron into the QR (QD). The first peak refers to the occupation of the first *s*-level. For the QD there are two *s* and *p*-shells of the electron levels below the bottom of GaAs conduction band [1–3]. The first level of the *d*-shell is located above this threshold, and is not observed. Nevertheless, in a weak magnetic field the d-level appears in the spectrum due to the orbital Zeeman effect [1,4]. Therefore we can define the energy of the s-level in respect to the bottom of GaAs conduction band. Recalculation of the gate-voltage to energy can be done by using the voltage-to-energy conversion coefficient $f = (e\Delta V)/\Delta E$ which is equal to 7 [1]. For the QR we found that the *s*-level is located approximately 30 meV below the potential barrier E_0. The excitation energies calculated at various strengths of the magnetic field B, together with experimental data for a single tunneled electron [3], are shown in figure 4. In experiments [2–3] only the resonances with the change in the orbital quantum number $|\Delta l| = 1$ were measured. Such resonances were calculated and are shown in figure 4, as connected by the solid lines. The lines diverging from the point $B = 0$ exhibit the orbital Zeeman splitting for the non-zero electron levels with the magnetic field increase. The agreement between our results and the experiment is quite satisfactory.

The effect of the non-parabolicity, taken into the account in our model, leads to a significant change in the electron effective mass of the QR in respect to the bulk value (according to the relation (2)). For the QR considered above the effective mass of InAs increases from the initial bulk value of 0.024 m_0 to 0.0615 m_0, which is numerically close to the electron effective mass of 0.063 m_0 obtained in FIR experiments [2–3] from the orbital Zeeman splitting. One can see that our calculations differ from the results obtained by using the planar model [3], in particular, in the magnitude of the period of the electron ground state orbital number transfer in a magnetic field. The calculated first change of l from 0 to -1 occurs at $B \sim 3$ T, whereas according to Ref. [3], it happens at $B \sim 7$ T. This fact can be understood by considering the relationship between the energy and the magnetic flux Φ for an ideal QR [14] of radius R_0 in the normal magnetic field:

$$E_{(0,1)} = \hbar^2/\left(2m^* R_0^2\right)(l + \Phi/\Phi_0)^2, \qquad (3)$$

where $\Phi = \pi R_0^2 B$ is the magnetic flux quantum, Φ_0 is the magnetic flux quantum ($\Phi_0 = 4135.7$ T nm), and e is the electron charge. The relation (3) is approximately holding true in our model, as it shown in table 1, where the energies of a first few electron levels and the magnitude

Table 1. Electron excitation energy $\Delta E_{(0,l)}$, $l = 1, 2, 3$, (in meV) calculated in presented 3D model, and the ideal ring model. The Aharonov–Bohm period ΔB for each model is shown.

Model	$\Delta E_{(0,1)}$	$\Delta E_{(0,2)}$	$\Delta E_{(0,3)}$	ΔB, T
3D model	2.8	9.3	17.4	6.0
Ideal ring model	2.5	9.9	22.3	5.3

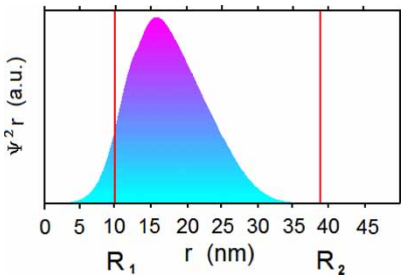

Figure 5. Projection of the electron wave function $\Psi^2 r$ on the plane normal to the z-axis. The locations of the inner R_1 and the outer R_2 radii of the quantum ring are shown.

of the Aharonov–Bohm period [14] obtained from our model and by the model of ideal ring equation (3) are presented. Note that the Aharonov–Bohm period is defined as a value of the magnetic field for the orbital number transfer $|\Delta l| = 1$, and it is calculated by the expression: $\Delta B = \Phi_0/(\pi R_0^2)$. For the ideal ring calculation the value of the radial variable r at the maximum of the electron wave function $\Psi^2(r,z)r$ is used as the radius of the ring R_0. One can see in figure 5 that R_0 is about 16 nm. It is clear that the correspondence between 3D model and the ideal ring model can only be defined after calculation of the radial variable r at the maximum of the electron wave function in framework of the 3D model.

The value of $R_0 = 14$ nm in the model [2,3] corresponds to a minimum of the parabolic confinement potential. The relation $E_{(0,1)} = \hbar^2/(2m^* R_0^2)(l + \Phi/(2\Phi_0))^2$ is applicable in this case, and can be interpreted as that the model [2,3] provides the value of 2 Φ_0 for magnetic flux quantum.

5. Conclusions

InAs/GaAs QR was studied under the energy dependent effective mass approximation. It is found that the incorporation of the effective potential, simulating a total effect of the band-gap deformation potential, the strain induced potential, and the piezoelectric potential into a model of the QR, allows a reasonable interpretation of experimental data for single electron levels. It is shown that the observed deviation of the electron effective mass of the QR from its bulk value can be attributed to the non-parabolic effect. The effect of the 3D geometry of QR on the energy of electron levels and the Aharonov–Bohm period was evaluated by a comparison with the ideal ring model. We have found that the one dimension ideal ring model can be used for qualitative description of the experiment data. However, this model needs to include a parameter which can be accurately defined in the 3D model only.

Acknowledgements

This project is supported by the Department of Defense through grant No. DAAD 19-01-1-0795. I.F. also is partly supported by NASA grant NAG3-804.

References

[1] B.T. Miller, *et al.* Few-electron ground states of charge-tunable self-assembled quantum dots. *Phys. Rev. B*, **56**, 6764 (1997).
[2] A. Lorke, R.J. Luyken, A.O. Govorov, J.P. Kotthaus, J.M. Garcia, P.M. Petroff. Spectroscopy of nanoscopic semiconductor rings. *Phys. Rev. Lett.*, **84**, 2223 (2000).
[3] A. Emperador, M. Pi, M. Barranko, A. Lorke. Far-infrared spectroscopy of nanoscopic InAs rings. *Phys. Rev. B*, **62**, 4573 (2000).
[4] R.J. Warburton, B.T. Miller, C.S. Durr, C. Bodefeld, K. Karrai, J.P. Kotthaus, G. Medeiros-Ribeiro, P.M. Petroff, S. Huant. Coulomb interactions in small charge-tunable quantum dots: a simple model. *Phys. Rev. B*, **58**, 16221 (1998).
[5] S.S. Li, J.B. Xia. Electronic states of InAs/GaAs quantum ring. *J. Appl. Phys.*, **89**, 3434 (2001).
[6] J.I. Climente, J. Planelles, F. Rajadell. Energy structure and far-infrared spectroscopy of two electrons in a self-assembled quantum ring. *J. Phys. Condens. Matter*, **17**, 1573 (2005).
[7] E. Kane. Band structure of indium antimonide. *J. Phys. Chem. Solids*, **1**, 249 (1957).
[8] R. Blossey, A. Lorke. Wetting droplet instability and quantum ring formation. *Phys. Rev. E*, **65**, 021603 (2002).
[9] Y. Li, O. Voskoboynikov, C.P. Lee, S.M. Sze, O. Tretyak. Electron energy state dependence on the shape and size of semiconductor quantum dots. *J. Appl. Phys.*, **90**, 6416 (2002).
[10] I. Filikhin, E. Deyneka, B. Vlahovic. Energy dependent effective mass model of InAs/GaAs quantum ring. *Modelling Simul. Mater. Sci. Eng.*, **12**, 1121 (2004).
[11] A.O. Govorov, S.E. Ulloa, K. Karrai, R.J. Warburton. Polarized excitons in nanorings and optical Aharonov–Bohm effect. *Phys. Rev. B*, **66**, 081309(R) (2002).
[12] I. Filikhin, E. Deyneka, B. Vlahovic. Single-electron levels of InAs/GaAs quantum dot: comparison with capacitance spectroscopy. *Physica E*, **31**, 99 (2006).
[13] M. Levinshtein, S. Rumyantsev, M. Shur (Eds.). *Handbook Series on Semiconductor Parameters*, World Scientific, Singapore (1999).
[14] A.G. Aronov, Yu.V. Sharvin. Magnetic flux effects in disordered conductors. *Mod. Phys.*, **59**, 755 (1987).